PROTOTYPING HIGH-GRADIENT mm-WAVE ACCELERATING STRUCTURES *

E. A. Nanni[†], V. A. Dolgashev, A. Haase, J. Neilson,
S. Tantawi, SLAC National Accelerator Laboratory, Menlo Park, USA
S. C. Schaub, R. J. Temkin, Massachusetts Institute of Technology, Cambridge, USA
B. Spataro, INFN-LNF, Frascati, Rome, Italy

Abstract

We present single-cell accelerating structures designed for high-gradient testing at 110 GHz. The purpose of this work is to study the basic physics of ultrahigh vacuum RF breakdown in high-gradient RF accelerators. The accelerating structures are π-mode standing-wave cavities fed with a TM_{01} circular waveguide. The structures are fabricated using precision milling out of two metal blocks, and the blocks are joined with diffusion bonding and brazing. The impact of fabrication and joining techniques on the cell geometry and RF performance will be discussed. First prototypes had a measured Q_0 of 2800, approaching the theoretical design value of 3300. The geometry of these accelerating structures are as close as practical to single-cell standing-wave X-band accelerating structures more than 40 of which were tested at SLAC. This wealth of X-band data will serve as a baseline for these 110 GHz tests. The structures will be powered with short pulses from a MW gyrotron oscillator. RF power of 1 MW may allow an accelerating gradient of 400 MeV/m to be reached.

INTRODUCTION

The high-gradient performance of accelerating structures is important for the selection of an accelerator's operational frequency. RF breakdown is one of the major phenomena that limits the achievable gradient in accelerating structures. Extensive studies on RF breakdown in copper accelerating structures [1] have been performed at frequencies as high as 11-12 GHz [2–6], 17 GHz [7] and 30 GHz [8–10].

The statistical behavior of RF breakdown became apparent during NLC/GLC work [2, 4, 11, 12]. After many pulses at the same RF power and pulse shape, for most accelerating structures the breakdown rate approached a steady state or is slowly decreasing. It is now common practice to measure and use the breakdown probability to quantify the high-gradient performance of accelerating structures.

Recently, we have expanded our experiments on the basic physics of ultrahigh vacuum RF breakdown to the mm-wave range with beam-driven accelerators at FACET [13, 14]. In this paper, we continue this study [15] using a 110 GHz MW pulsed gyrotron oscillator [16] as the RF power source. We are aiming to achieve accelerating gradients well beyond 100 MeV/m and plan to measure RF breakdown statistics.

ACCELERATING STRUCTURE DESIGN

We are designing standing-wave accelerating structures with cavity geometries that allow for direct comparison with experiments at 11.424 GHz conducted at the SLAC National Accelerator Laboratory [3], where accelerating cavities with a/λ ratios of 0.105, 0.143 and 0.215 were extensively studied. Here a is the radius of the iris aperture and λ is the operational wavelength. Structures with a larger a/λ have a higher peak surface electric field for the same accelerating gradient. For our experiments we are designing cavities with the same a/λ ratios.

We presented the detailed design of the 110 GHz structures in [15]. These structures have three cells, with the on-axis electric field in the central cell twice as high as in the adjacent cells. This was done to ensure that most of the breakdowns are in the central cell. The two end cells create fields that mimic the fields in a multi-cell standing wave structure. The on-axis electric fields for several values of a/λ are shown in Fig. 1. The accelerating structure is fed through a 1.187 mm radius TM_{01} cylindrical waveguide. The beam pipe radius is 0.660 mm radius so the TM_{01} mode is below cutoff. The RF parameters of the three structures are given in Table 1. The parameters were normalized for 1 MW of dissipated RF power.
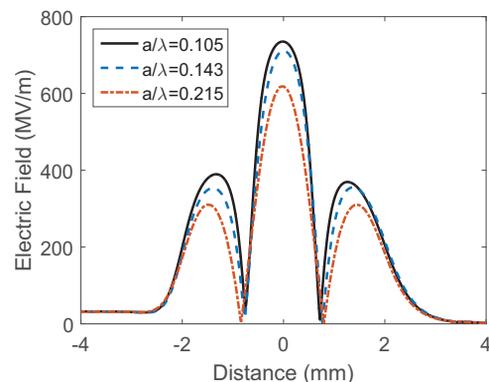
Figure 1: On-axis electric field for three cavities with different a/λ assuming 1 MW of dissipated RF power in the structure.

We plan to use a 110 GHz 1 MW gyrotron to power our accelerating structures. The RF power is transported to the accelerating structure in a free-space Gaussian mode. We couple the RF power into the accelerating structure using a Gaussian to TM_{01} mode converter. The mode converter is shown in Fig. 2. First, the Gaussian mode is focused

Table 1: RF parameters of 110 GHz single-cell accelerating structures. Fields are normalized to 1 MW of dissipated RF power. Accelerating gradient is defined as the peak surface electric field divided by K_e which was determined for the periodic solution [15].

Name	Unit	A0.286-T0.2-Cu	A0.390-T0.2-Cu	A0.586-T0.4-Cu
a/λ		0.105	0.143	0.215
Iris Aperture Radius, a	[mm]	0.286	0.390	0.586
Iris Thickness, t	[mm]	0.2	0.2	0.4
Iris Ellipticity		1	1.35	1.3
Accelerating Gradient, E_{acc}	[MeV/m]	404	361	277
Max. Surface Elec. Field, E_{max}	[MV/m]	916	827	624
Max. Surface Mag. Field, H_{max}	[MA/m]	1.13	1.13	1.16
$H_{max}Z_0/E_{acc}$		1.04	1.13	1.47
$K_e = E_{max}/E_{acc\text{-}periodic}$		2.27	2.29	2.25
Peak Pulsed Heating (20 ns Square Input Pulse)	[^{o}C]	156	156	165

onto the aperture of a smooth-walled horn with ~6 mm beam waist. The horn converts the Gaussian mode into the TE_{11} mode of a circular waveguide with ~99% conversion efficiency. Following the Gaussian converter is a TE_{11} to TM_{01} mode converter, which includes a 90 degree bend. The mode converter has a 97% power conversion efficiency and a bandwidth exceeding 2 GHz. The parameters of the mode converter exceed the requirements for this experiment since its bandwidth is larger than the tunable frequency range of the gyrotron oscillator.
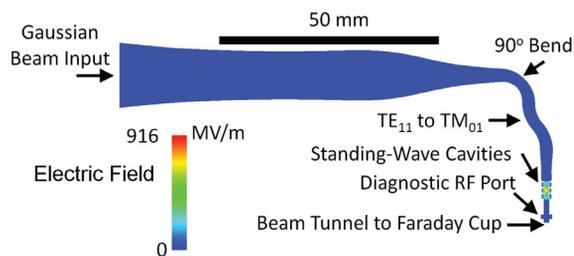
Figure 2: Model of the assembly consisting of the mode converter and the standing-wave accelerating structure A0.286-T0.2-Cu. We show the magnitude of the electric field on the symmetry plane using HFSS [17]. The field is normalized for 1 MW in the input Gaussian beam.

PROTOTYPE STRUCTURES

For rapid prototyping we created simplified structures with geometries similar to our final accelerating structures. These structures consist of three identical cells with beam pipes at each end. The structures are made in halves, where each half is milled into a copper block as shown in Fig. 3. Then the two halves are joined together with bonding and/or brazing. We call this the "split-cell" fabrication technique. The split interface is parallel to the RF currents of the operating mode, thus the ohmic Q factor of the structures is determined by the properties of the surface and not the interface.

We measured the RF properties of the prototypes with a vector network analyzer and two coaxial probes inserted into the beam pipes. The structures were cold tested both before and after bonding.

Of particular interest for us was the Q factor value and its repeatability, the repeatability of resonant frequency between multiple structures machined in a single milling operation, and the frequency difference before and after bonding. The consistency of the resonant frequency between prototypes was considered a secondary objective, with the absolute frequency of the cavities was required to be close to our final target of 110 GHz. To date, 15 RF structures have been fabricated in 5 split-cell assemblies with three structures each.
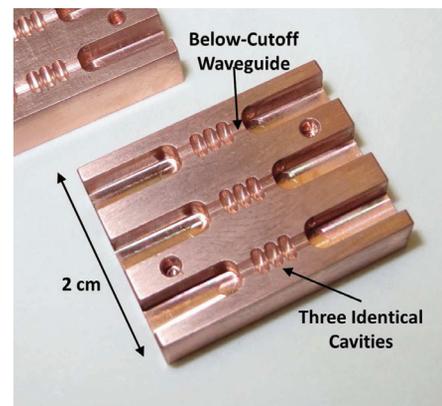
Figure 3: Photograph of a milled copper block with three halves of the accelerating structure.

We found that both the diffusion bonding and brazing were able to produce cavities with Q factors of 2700-2800 for the π-mode, approaching the theoretical expectation of 3300. Post bonding autopsy showed significant variation of the interface structure between brazing and diffusion bonding, see Fig. 4. Due to the orientation of this interface with respect to RF currents this variation has little effect on Q value and resonant frequency. With the correct amount of

braze alloy, interfaces were sealed uniformly through the iris (Fig. 4(left)). However, we observed a gap in the iris with diffusion bonding (Fig. 4(right)). While the gap did not result in a degradation of RF parameters, the exposed corners may result in local electric field enhancement. We speculate that this enhancement may affect the high-gradient performance of the cavity. In this particular assembly, we see a misalignment between the two diffusion bonded blocks at the interface. Unlike prototypes, in the high power assembly we placed a stricter tolerance on the alignment between the two blocks.
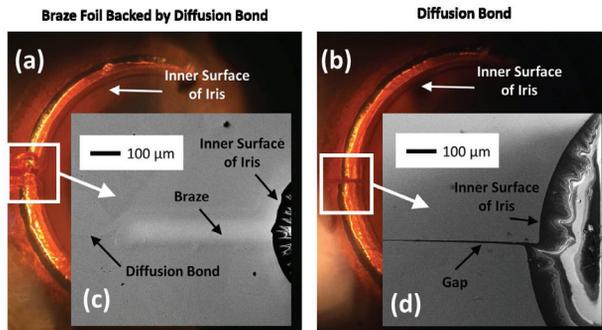
Figure 4: Photograph of (a) brazed and (b) diffusion bonded iris with a=1.02 mm. SEM image of the same (c) brazed and (d) bonded joints machined down to the middle of the iris in order to show the internal mechanical structure.

Diffusion bonded and brazed cavities had a mean π-mode resonant frequency of 107.69 GHz, with a standard deviation of 210 MHz over all 15 cavities. Between the three structures in the same split-cell assembly the deviation was much smaller, 60 MHz on average. We observed a significant frequency increase between pre-bonding and after bonding measurements, with a mean of 430 MHz and a standard deviation of 190 MHz. We did not see a significant correlation in the frequency shift with the bonding technique. We note that both the brazing and the diffusion bonding procedure include cleaning with chemical etching. We speculate that the cavity deformation from this bonding procedure is the dominant source of the frequency shift. Understanding and controlling this frequency shift is an objective of the ongoing study.

HIGH POWER STRUCTURE

Two high power RF structures from Fig. 2 were fabricated in both copper (Cu) and copper-silver (CuAg) by EDM Department, Inc. In Fig. 5 we show a photograph of one half of the Cu structure. These structures will be diffusion bonded. The measured π-mode frequency of the clamped structures is 109.503 GHz for Cu and 109.254 GHz for CuAg. We performed S-parameter measurements of the clamped assembly, with the S_{11} vs. frequency is shown in Fig. 5. We measured a loaded Q factor of 1600 for Cu and 1200 for CuAg structures. These are in good agreement with the expected loaded Q factor of 1800. The spacing of the 0 and π modes does not match the design due to variations in cell coupling, however

it is acceptable and will not impact the high power test. In future we also plan to build brazed assemblies.
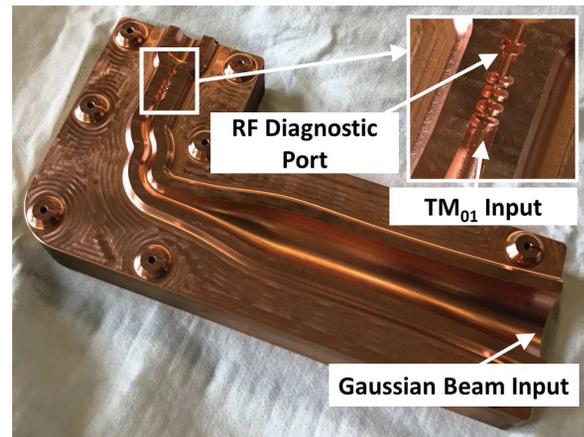
Figure 5: Photograph of one half of the high-power split-cell structure.
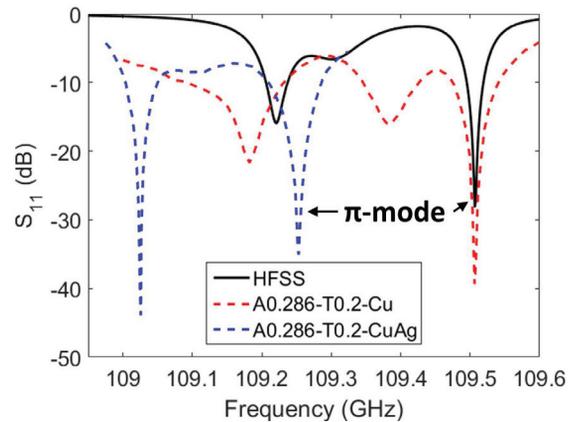
Figure 6: Simulated and measured S_{11} for the Gaussian beam mode converter and the high-power accelerating structure. The HFSS simulation is shifted down by 600 MHz from the nominal frequency to align the frequencies of the π-mode for the Cu structure. We expect that bonding will shift the π-mode frequency up by at least 400 MHz.

CONCLUSION

We have presented single-cell accelerating structures designed for high-gradient testing at 110 GHz using a gyrotron as the RF power source. We built 5 split-cell prototypes with three structures each to test manufacturing techniques. We built two high-power structures one of Cu and another one of CuAg. Cold tests indicate that the desired RF parameters could be achieved. With 1 MW these structures may reach peak accelerating gradients of 400 MeV/m.

ACKNOWLEDGMENT

REFERENCES

[1] Chang, Chao, et al., "Review of recent theories and experiments for improving high-power microwave window breakdown thresholds", *Physics of Plasmas*, 18.5 (2011): 055702.

[2] Döbert, Steffen, et al., "High gradient performance of NLC/GLC X-band accelerating structures", in *Proc. of IPAC 2005*, Knoxville, Tennessee, 2005, pp. 372-374.

[3] Dolgashev, Valery, et al., "Geometric dependence of radio-frequency breakdown in normal conducting accelerating structures", *Applied Physics Letters*, 97.17 (2010): 171501.

[4] Higo, Toshiyasu, et al., "Advances in X-band TW Accelerator Structures Operating in the 100 MV/m Regime", in *Proc. of IPAC 2010*, Kyoto, Japan, THPEA013, (2010), p. 3702.

[5] Marsh, Roark A., et al., "X-band photonic band-gap accelerator structure breakdown experiment", *Physical Review Special Topics-Accelerators and Beams*, 14.2 (2011): 021301.

[6] Degiovanni, A., et al., "High-Gradient Test Results From a CLIC Prototype Accelerating Structure: TD26CC", in *Proc. of IPAC2014*, Dresden, Germany, WEPME015. 2014.

[7] Munroe, Brian J., et al., "Experimental high gradient testing of a 17.1 GHz photonic band-gap accelerator structure", *Physical Review Accelerators and Beams* 19.3 (2016): 031301.

[8] Achard, C., et al., "30 GHz power production in CTF3", in *Proc. of IPAC 2005*, Knoxville, Tennessee, 2005, pp. 1695-1697.

[9] Rodriguez, J., et al., "30 GHz high-gradient accelerating structure test results", in *Proc. of PAC07*. Albuquerque, New Mexico, FROBC01, 2007.

[10] Grudiev, Alexej, S. Calatroni, and W. Wuensch, "New local field quantity describing the high gradient limit of accelerating structures", *Physical Review Special Topics-Accelerators and Beams* 12.10 (2009): 102001.

[11] J. W. Wang, "R&D of accelerator structures at SLAC", *High Energy Phys. Nucl. Phys.* 30, 11 (2006).

[12] C. Adolphsen, "Normal Conducting rf Structure Test Facilities and Results", in *Proceedings of the 2003 Particle Accelerator Conference*, Portland, OR (IEEE, New York,2003), p. 668.

[13] Dal Forno, Massimo, et al., "rf breakdown tests of mm-wave metallic accelerating structures", *Physical Review Accelerators and Beams* 19.1 (2016): 011301.

[14] Dal Forno, Massimo, et al., "High Gradient mm-Wave Metallic Accelerating Structures", *AIP Conference Proceedings* 1812, 060011 (2017).

[15] Nanni, Emilio, et al., "mm-Wave Standing-Wave Accelerating Structures for High-Gradient Tests", *7th International Particle Accelerator Conference (IPAC'16)* , Busan, Korea, May 8-13, 2016 (pp 3884-3887).

[16] Tax, David S., et al. "Experimental Results for a Pulsed 110/124.5-GHz Megawatt Gyrotron", *Plasma Science, IEEE Transactions on* 42.5 (2014): 1128-1134.

[17] ANSYS Electronics Desktop 16.2, *HFSS*.